SSRG International Journal of Mechanical Engineering
ISSN: 2348 – 8360 /doi:10.14445/23488360/IJME-V7I2P104
Volume 7 Issue 2, 21-25, February 2020


# Wind Turbine Applications in Doha Metro, Qatar

Yasin Furkan GORGULU[#1], Mustafa Arif OZGUR[*2], Ramazan KOSE[#3]

[#1,2,3]*Kutahya Dumlupınar University*
*Kutahya Dumlupinar University Faculty of Engineering, Department of Mechanical Engineering, Kutahya/Turkey*

***Abstract***

*In this study, a large amount of airflow is observed in the "Doha Metro" created by the trains' movement. Therefore, it is thought that waste, but a new potential can generate electrical energy. In literature, similar studies have been found in India, the US, and China. However, this project differs from others with various preferences such as turbine location and type sites. Horizontal axis wind turbines for the first scenario and vertical axis wind turbines are planned to be installed in spots where air properties such as pressure, velocity, and airflow are at their highest values. The turbines are considered to be installed on the tunnel walls' inner surface just between the train and the tunnel. For the study, Doha Metro's Red Line has been chosen as a reference line with the most potential compared to other lines. Energy generation has been computed, and the turbines have been installed in the cross-sectional area theoretically. Considering the actual industrial average price of electrical energy in Qatar, the energy generation's financial value has been calculated, and a feasibility study has been done.*

**Keywords —** *Wind turbine, electricity generation, metro.*

## I. INTRODUCTION

Considering Qatar's energy outlook, foremost natural gas and oil were the primary energy sources for electricity generation in 2018. Only a small amount of electricity was generated by renewable energy, which is lower than 1% [1]. In the future, due to the depletion of fossil fuels, Qatar may become dependent on other countries in terms of energy source imports. To outcome these threats, new potential sources might be used [2]. This study focuses on using existing but not used potentials. The idea is to generate electricity using the movement of the trains. The study's main aims are uncovering the hidden potentials and raising awareness all around the world.

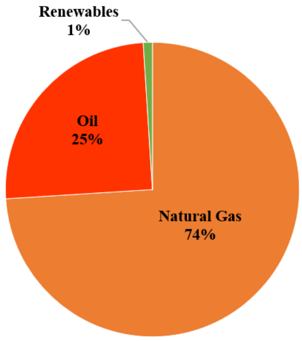


Fig 1.1. Primary energy consumption of Qatar in 2018 [1].

## II. MATERIALS AND METHODS

### A. Materials

#### *a) Doha Metro and defining the pilot line*

The pilot line (Red Line) has been made depending on several features that might positively or negatively affect the energy generation's effectiveness.

Table 2.1. Numerical values of the Doha Metro and the Red Line [3].

| Line | Colour | Inaugural date | Length | Stations | Termini | Current Stock | Status |
|---|---|---|---|---|---|---|---|
| Red Line | | 08.05.2019 | 40 km | 18 | Lusail<br>Hamad International Airport<br>Al Wakra | Mitsubishi Corporation<br>and<br>Kinki Sharyo | Al Qassar to Al Wakra now open. Hamad International Airport, Katara, Qatar University and Lusail stations expected to open in 2019. Lusail and Legtaifiya tram stations expected to open in 2020. |
| Green Line | | Expected 2019 | 22 km | 11 | Al Riffa<br>Al Mansoura | Mitsubishi Corporation<br>and<br>Kinki Sharyo | Undergoing final safety and security tests. |
| Gold Line | | Expected 2020 | 14 km | 11 | Al Azizyah<br>Ras Bu Aboud | Mitsubishi Corporation<br>and<br>Kinki Sharyo | |
| Total | | | 76 km | 40 | | | |

The features such as the length of the deep tube, annual train count, station number have been considered, and "Red Line" that bears the highest energy generating capacity. Furthermore, the technical suitability of the Red Line also supports the project. From table 2.1., it can be seen that the Red Line has a deep tube with a length of 40 km, 18 stations. What is more, rolling stock sizes of Red Line trains can be accessible (Table 2.1. and figure 2.1).

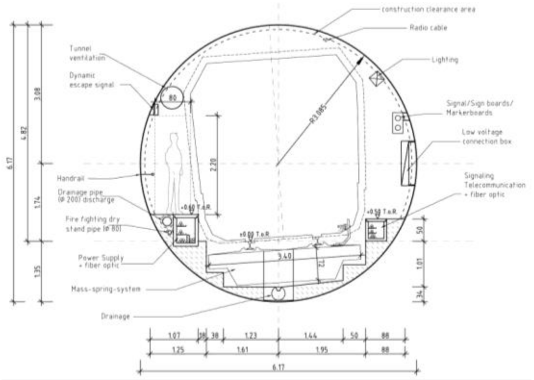


Figure 2.1. Doha Metro and tunnel cross-section [3].

***b) Geometrical suitability approach***

The first step of the geometrical suitability approach is to calculate train and tunnel geometries by reducing its parts into calculable geometrical parts. 2 methods have been taken into account to find the cross-sectional areas. The first method is less sensitive when it is compared to the second method. In table 2.2, the cross-sectional area is divided into several geometrical shapes. Then the dimensions and the area of the shapes approximated and calculated, respectively. Table 2.2. demonstrates the calculations made for the geometrical suitability approach [4].

Table 2.2. Train and tunnel illustration with geometrical parts and geometrical approach area.

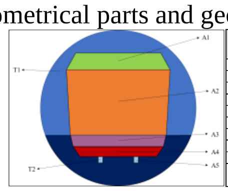


| Geometrical Part | Area of the Geometrical Part [m²] | Explanation |
|---|---|---|
| T1 | 21.74 | Upper Part of the Circle |
| T2 | 8.16 | Lower Part of the Circle |
| A1 | 2.16 | First Part of the Train |
| A2 | 8.12 | Second Part of the Train |
| A3 | 2.17 | Third Part of the Train |
| A4 | 1.38 | Fourth Part of the Train |
| A5 | 0.13 | Wheels of the Train |
| Cross Section | 29.9 | Tunnel |
| Cross Section | 13.96 | Train |
| Effective Area | 11.46 | The Gap Between the Train and Tunnel |

***c) Solid Works scaling approach***

The second method covers using a designing program called Solid Works (SW). On SW, a model of the train and the tunnel have been designed. Technical drawing of the train and tunnel has been taken, and on SW, it has been used to approximate not-given dimensions. Therefore, in further calculations, SW derived data have been used to have more accurate results. Figure 2.2. shows the scaling process and figure 2.2. illustrates the SW design progress.

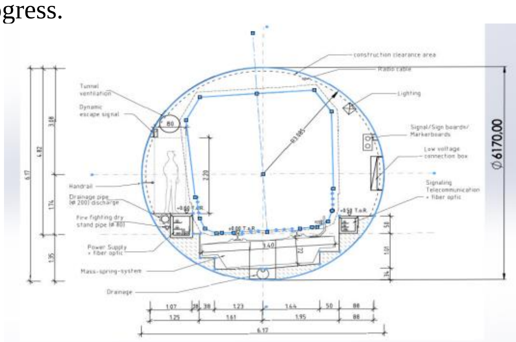


Figure 2.2. The technical drawing and the projection details of the pilot line [3].

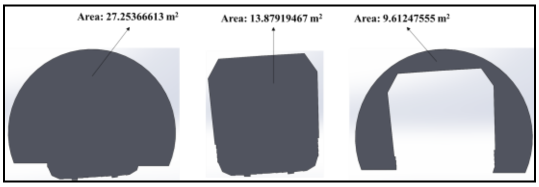


Figure 2.3. Tunnel and train's cross-sectional areas.

In the calculations, the flow velocity, in the gap between the tunnel and train (effective area), has been used. Table 2.3. summarises the figure changes between 2 approaches. SW Scaling Approach is more accurate; that is why those data are used in further calculations.

Table 2.3. Geometrical suitability and SW scaling approach comparisons

| Comparison Parameters | Unit | Geometrical Suitability Approach | Solid Works Approach |
|---|---|---|---|
| Cross-sectional Area of the Train | m² | 13.96 | 13.87919467 |
| Cross-sectional Area of the Tunnel | m² | 29.9 | 27.25366613 |
| Effective Area | m² | 11.46 | 9.61247555 |

Datasheet about Red Line and some of the calculations have been given in table 2.4.

Table 2.4. Numerical Values of the Doha Metro and Red Line [5].

| LINE | UNIT | RED LINE | EXPLANATIONS |
|---|---|---|---|
| Type | | Deep Tube | |
| Track Gauge | mm | 1435 | |
| Time between Adjacent Stations | minutes | 3 | |
| Headway | minutes | 5 | |
| Number of Passengers | billion/day | 600 | Passengers trips per day |
| TUNNEL | | | |
| Tunnel Inner Diameter | mm | 6170 | |
| System Length | km | 40 | |
| Number of Stations | No | 40 | |
| TRAIN | | | |
| Train Cross-sectional Area | m² | 13.96 | |
| Maximum Train Speed | km/h | 100 | |
| Maximum Train Speed | m/s | 27.7 | |
| Number of Cars | No | 3 | |
| Width of a Car | m | 3 | |
| Car Height | m | 4 | |
| CALCULATIONS | | | |
| Effective Cross-sectional Area | m² | 11.46 | |
| Average Distance between Two Stations | m | 2.14 | Total route/Number of Stations |
| Maximum Air Velocity to the Back | m/s | 40.1 | |

***d) Theoretical potential approach and calculations***

As the train enters a tunnel, a volume of air is created every time because of the train's motion in the tunnel. That volume of air is considered to move in the opposite direction that the train does. Calculations have been done in the direction of those principles. The flow velocity has been calculated with the help of the continuity equation, and it is assumed that the volume of the air is the same as the volume of the train is perpendicular to the train's movement direction, and it is also the opposite. As the created airflow moves in the opposite direction to the train, it will use the gap between the train and the tunnel to escape where wind turbines are installed. The friction losses have been taken as negligible losses, and therefore, the airflow discharged by the train is assumed to be the same as the airflow, which tries to escape through the train in the opposite direction. The airflow caused by the train's insertion in the tunnel is always equal to the airflow occurring between the tunnel and the train during the train's movement. It is assumed that there are no friction losses due to the air flows. Using the continuity equation allows us to find flow velocity between the train and the tunnel, which is needed for calculating the power generation of the turbines [6].

***e) Defining the suitable type of turbines***

The types of wind turbines have been chosen as new-generation wind jet type turbines. It is known that the efficiency of the wind jet type wind turbines is much higher than ordinary wind turbines. Apart from that advantage, it is also estimated that during the wind jet-type wind turbines, assembling and dissembling them would be easier [12]. Most wind turbines max out at 60% efficiency. The issue is that 40 per cent of the wind passes around the windmill's blades without actually turning the generator and making power. Here comes the FloDesign horizontal axis wind turbines and Aelos Brand vertical axis wind turbines to change all of that. By focusing the wind over the blades, it improves efficiency dramatically. They generate the same amount of power as a conventional windmill with double its size [12], [8]. This also means more wind turbines can be placed closer together, increasing output on a wind farm.

In consideration of tunnel-train geometry and the gap between the train and the tunnel, the wind turbines' theoretical settlement has been designed on a scaled technical drawing initially. To benefit from the maximum amount of energy generation rate, wind turbine sizes have been chosen in 4 types for the 1st scenario. As a result, 6 wind turbines with a diameter of 400 [mm], 3 wind turbines with a diameter of 600 [mm], 2 wind turbines with a diameter of 1000 [mm], and lastly, 2 turbines with a diameter of 1200 [mm] have been installed. For the 2nd scenario, 2 different sized wind turbines have been chosen. 2 wind turbines with a diameter of 900 [mm] and 2100 [mm] height and a turbine with a diameter of 2000 [mm] and 450 [mm] height. The designed wind turbine layout is given in the picture below (Figure 2.4. and 2.5.).

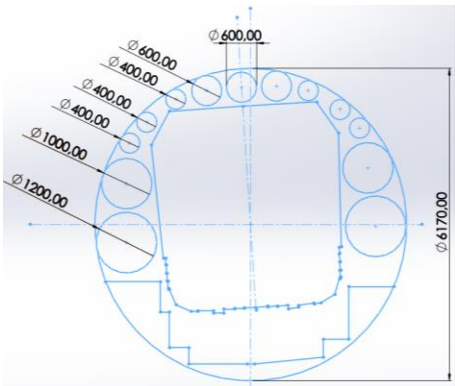


Figure 2.4. The layout of the horizontal axis wind turbines, train, and tunnel.

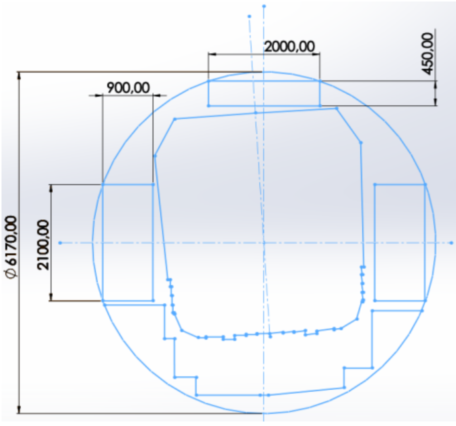


Figure 2.5. The layout of the vertical axis wind turbines, train, and tunnel.

## III. RESULTS, CONCLUSIONS AND RECOMMENDATIONS

***A. Technical results and applicability***

Considering the reference line's data, the train's intensive movement (a train in 3 minutes), and the train's speed, it can be seen from the velocity calculations that a high proportion of airflow occurs. When all of the train's losses are neglected, it is calculated that airflow velocity can go up to 40.1 m/s whenever the train reaches 100 km/h. That velocity might exceed the limit of conventional wind turbines (most of them can withstand up to 20 m/s), which is why wind turbines are considered to be used in the project wind jet-type wind turbines. What is more, these wind turbines are also more efficient than conventional wind turbines. The efficiency contrast between them is considerable, while conventional turbines have 35 % efficiency, wind jet type wind turbines possess 45 % efficiency [4]. Horizontal axis wind turbines mostly suit the project's idea, and therefore, horizontal axis wind turbines are thought to be installed in the gap between the train and the tunnel. The gap between the train and tunnel, the dimensions of the train and the tunnel, and other found dimensions have been scaled up in a technical drawing with the help of the SW engineering designing program, and the not-found sizes have been tried to be determined. On the technical drawing, 13 wind turbines with 4 different diameters for the 1st and the 2nd scenario 3 wind turbines with 2 different diameters have been installed (see Figure 2.4.). The model's unique side is that from one set of turbines, it is possible to generate 119,071 kWh from the 1st scenario and 104,794 kWh electrical energy from the 2nd scenario every year. In the calculations, in case of malfunctions and maintenance, the wind turbines' operation duration has been taken as 300 days instead of 365 days. The generated energy can be stored in batteries; however; there is also another option, which is called grid-off system. Grid off system does not require the electrical energy stored. It directly uses the generated electrical energy, and therefore, the energy is considered to be used directly in the lighting and ventilation of the metro stations [4]. What is more, the grid off system's total cost is also less risky and expensive than the other option with batteries. To calculate the generation of electricity, Betz Limit, or Betz' Law has been used [6]. The calculation chart has been given in table 3.1.

Table 3.1. Calculation Chart [9].

| Formula | Calculation Result | Unit | Explanations |
|---|---|---|---|
| $v_a = v_0 \pm a_a \times t_{acc}$ | $t_{acc} = 17.09$ | s | Acceleration time |
| $x_{acc} = v_0 \times t_{acc} \pm 1/2 \times a_{acc} \times t_{acc}^2$ | $x_{acc} = 189.84$ | m | Acceleration distance |
| $v = v_0 - a_{dec} \times t_{dec}$ | $t_{dec} = 19.5$ | s | Deceleration time |
| $x_{dec} = v_0 \times t_{dec} \pm 1/2 \times a_{dec} \times t_{dec}^2$ | $x_{dec} = 216.54$ | m | Deceleration distance |
| $x_{acc} + x_{dec}$ | 406,38 | m | Total acceleration and deceleration distance |
| $x_m = 1160 - (x_{acc} - x_{dec})$ | $x_m = 753.62$ | m | The train moves at maximum speed among this distance |
| $t_m = x/v = x_{dec}/v$ | $t_m = 33.916$ | s | Time apart from acceleration and deceleration (The train moves at maximum speed in this time interval) |
| $P_{a1} = (½) \times A_v \times \rho \times C_p \times V^3$ | $P_{a1} = 119{,}071$ | kWh | Annual electricity generation (1st scenario) |
| $P_{a2} = (½) \times A_v \times \rho \times C_p \times V^3$ | $P_{a2} = 104{,}794$ | kWh | Annual electricity generation (2nd scenario) |

## B. *Financial results*

The calculated amount of the energy (119,071 kWh and 104,794 kWh) is based on Qatar's industrial electricity tariff, and thus, the annual income has been calculated. (Table 3.2.) The industrial price of electricity per unit has been taken as 0,13 Qatari Rial (QR) [10], and annual income has been calculated as 15,480 QR however; for this scenario, 98,900 QR for 1st and 87,500 QR is needed for the investment. In the feasibility study, the net present value is assumed as 3.5 % [4]. As the economic lifetime of the turbines and equipment, 10, 15, 20 years have been taken in the financial calculations, and in the literature, it is pointed out that the lifetime of the turbines and equipment is taken as 20 years [8]. As an amortization method, the accelerated amortization method has been used in the calculations, and 50 per cent of the amortization expenses have been taken into account. In the direction of the assumptions mentioned above, feasibility calculations can be pointed out in table 3.2.

Table 3.2. Feasibility Results for the 1st and 2nd scenario, respectively [11].

| Parameters | Formulas | Results |
|---|---|---|
| **Return on Investment (ROI)** | $\text{ROI} = \frac{\text{Net Income} \times (\text{Gains} - \text{Costs})}{\text{Costs}}$ | 164,23% |
| **Payback Period (PP)** | $\text{Payback Period} = \frac{\text{Cost of Investment}}{\text{Annual Cash Flows}}$ | 6.38 Years |
| **Internal Rate of Return (IRR)** | $0 = R_0 + \frac{R_1}{1+\text{IRR}} + \frac{R_2}{(1+\text{IRR})^2} + \frac{R_3}{(1+\text{IRR})^3} + \cdots + \frac{R_n}{(1+\text{IRR})^n}$ | 14,72% |
| **Net Present Value (NPV)** | $\text{NPV} = \frac{R_1}{(1+i)^1} + \frac{R_1}{(1+i)^1} + \cdots + \frac{R_1}{(1+i)^n} - C$ | 81,000 QR |

| Parameters | Formulas | Results |
|---|---|---|
| **Return on Investment (ROI)** | $\text{ROI} = \frac{\text{Net Income} \times (\text{Gains} - \text{Costs})}{\text{Costs}}$ | 159,40% |
| **Payback Period (PP)** | $\text{Payback Period} = \frac{\text{Cost of Investment}}{\text{Annual Cash Flows}}$ | 6.42 Years |
| **Internal Rate of Return (IRR)** | $0 = R_0 + \frac{R_1}{1+\text{IRR}} + \frac{R_2}{(1+\text{IRR})^2} + \frac{R_3}{(1+\text{IRR})^3} + \cdots + \frac{R_n}{(1+\text{IRR})^n}$ | 15,01% |
| **Net Present Value (NPV)** | $\text{NPV} = \frac{R_1}{(1+i)^1} + \frac{R_1}{(1+i)^1} + \cdots + \frac{R_1}{(1+i)^n} - C$ | 77,000 QR |

With the increase of 10 % in NPV and PP, the highest value is found for the income, which means the income rises, NPV and PP are affected positively. To conclude, from a financial perspective, changes in the cost of the investment and the amount of income influence the results extremely. As a result, the feasibility result is affected by the cost of the investment and the amount of income. A summarised generated electricity calculation chart has been given in table 3.3. At 17.1, the train completes its acceleration, and until 51st second, the train keeps the same speed. Just after 51st second, the deceleration starts, and the train slows down. At 56th second, the train starts to leave the tunnel.

Table 3.3. Generated electricity calculation chart for 1st and 2nd scenario, respectively [11].

| Air Flow and Generated Power Calculation Chart | | | | | | | | | $P_a = (1/2) \times A_v \times \rho \times C_p \times V^3$ | | | |
|---|---|---|---|---|---|---|---|---|---|---|---|---|
| **Turbine Diameter (mm)** | **Air Density (kg/m³)** | **Cross-Sectional Area of Tunnel (m²)** | **Cross-Sectional Area of Train (m²)** | **Effective Area (m²)** | **Train Speed (m/s)** | **Blade Swept Area (m²)** | **Flow Velocity (m/s)** | **Power Coefficient** | **Generated Power; Pa (Wh)** | **Time (s)** | **No of Turbines** | **Total Power (Wh/Cycle)** |
| **400** | 1.122 | 29.9 | 13.96 | 11.46 | 13.85 | 0.1256 | 16.8713 | 0.45 | 152.3480 | 17.09 | 6 | 4.3393 |
| **400** | 1.122 | 29.9 | 13.96 | 11.46 | 27.7 | 0.1256 | 33.7427 | 0.45 | 1.2187 | 33.9066 | 6 | 68.8747 |
| **400** | 1.122 | 29.9 | 13.96 | 11.46 | 13.85 | 0.1256 | 16.8713 | 0.45 | 152.3480 | 19.49 | 6 | 4.9487 |
| **600** | 1.122 | 29.9 | 13.96 | 11.46 | 13.85 | 0.2827 | 16.8713 | 0.45 | 342.7831 | 17.09 | 3 | 4.8818 |
| **600** | 1.122 | 29.9 | 13.96 | 11.46 | 27.7 | 0.2827 | 33.7427 | 0.45 | 2.7422 | 33.9066 | 3 | 77.4840 |
| **600** | 1.122 | 29.9 | 13.96 | 11.46 | 13.85 | 0.2827 | 16.8713 | 0.45 | 342.7831 | 19.49 | 3 | 5.5673 |
| **1.000** | 1.122 | 29.9 | 13.96 | 11.46 | 13.85 | 0.7853 | 16.8713 | 0.45 | 952.17544 | 17.09 | 2 | 9.0403 |
| **1.000** | 1.122 | 29.9 | 13.96 | 11.46 | 27.7 | 0.7853 | 33.7427 | 0.45 | 7.6174 | 33.9066 | 2 | 143.4890 |
| **1.000** | 1.122 | 29.9 | 13.96 | 11.46 | 13.85 | 0.7853 | 16.8713 | 0.45 | 491.6319 | 19.49 | 2 | 5.3232 |
| **1.200** | 1.122 | 29.9 | 13.96 | 11.46 | 13.85 | 1.1309 | 16.8713 | 0.45 | 1.3711 | 17.09 | 2 | 13.0181 |
| **1.200** | 1.122 | 29.9 | 13.96 | 11.46 | 27.7 | 1.1309 | 33.7427 | 0.45 | 10.969 | 33.9066 | 2 | 206.6242 |
| **1.200** | 1.122 | 29.9 | 13.96 | 11.46 | 13.85 | 1.1309 | 16.8713 | 0.45 | 707.9500 | 19.49 | 2 | 7.6655 |

| | | |
|---|---|---|
| Total Power (Wh/1 pass) | 551.2567 | 33 Turbines/set |
| Total Power (Wh) | 16,537.7010 | A train in two min |
| Total Power (kWh/day) | 396.9048 | 24 Hours |
| Total Power (kWh/annum) | 119,071.4477 | 300 days/year |

| Air Flow and Generated Power Calculation Chart | | | | | | | | | | $P_a = (1/2) \times A_v \times \rho \times C_p \times V^3$ | | | |
|---|---|---|---|---|---|---|---|---|---|---|---|---|---|
| **Turbine Diameter (mm)** | **Turbine Height (mm)** | **Air Density (kg/m³)** | **Cross-Sectional Area of Tunnel (m²)** | **Cross-Sectional Area of Train (m²)** | **Effective Area (m²)** | **Train Speed (m/s)** | **Blade Swept Area (m²)** | **Flow Velocity (m/s)** | **Power Coefficient** | **Generated Power; Pa (Wh)** | **Time (s)** | **No of Turbines** | **Total Power (Wh/Cycle)** |
| **900** | **2100** | 1.122 | 29.9 | 13.96 | 11.46 | 13.85 | 1.89 | 16.8713 | 0.45 | 2291.3366 | 17.09 | 2 | 21.7549 |
| **900** | **2100** | 1.122 | 29.9 | 13.96 | 11.46 | 27.7 | 1.89 | 33.7427 | 0.45 | 18330.6931 | 33.9066 | 2 | 345.2952 |
| **900** | **2100** | 1.122 | 29.9 | 13.96 | 11.46 | 13.85 | 1.89 | 16.8713 | 0.45 | 2291.3366 | 19.49 | 2 | 24.8100 |
| **2000** | **450** | 1.122 | 29.9 | 13.96 | 11.46 | 13.85 | 0.9 | 16.8713 | 0.45 | 1091.1126 | 17.09 | 1 | 5.1797 |
| **2000** | **450** | 1.122 | 29.9 | 13.96 | 11.46 | 27.7 | 0.9 | 33.7427 | 0.45 | 8728.9015 | 33.9066 | 1 | 82.2131 |
| **2000** | **450** | 1.122 | 29.9 | 13.96 | 11.46 | 13.85 | 0.9 | 16.8713 | 0.45 | 1091.1126 | 19.49 | 1 | 5.9071 |

| | | |
|---|---|---|
| Total Power (Wh/1 pass) | 485.1603 | 33 Turbines/set |
| Total Power (Wh) | 14,554.8118 | A train in two min |
| Total Power (kWh/day) | 349.3154 | 24 Hours |
| Total Power (kWh/annum) | 104,794.6456 | 300 days/year |

## C. *Recommendations*

- There are several potentials to generate electrical energy from off-shore and in-shore sources in the world and Qatar.
- The airflow potential to produce electrical energy seems useful for the undergrounds.
- It is needed to be simulated one of the turbines in the metro as a prototype to measure and define the electrical energy generation's potential in the underground metros.
- It is needed that the new generation jet type turbines to test and to define their precise efficiency and suitability.

## ACKNOWLEDGMENTS

I want to express my thanks to Mustafa Arif OZGUR, Ramazan KOSE, for their guidance while writing the paper and to Ahmet GORGULU for his support and foresight processes.

## REFERENCES

[1] BP Statistical Review of World Energy Statistical Review of World, Ed. BP Stat. Rev. World Energy. (2019) 1–69.

[2] M. A. Kunt, İçten Yanmalı Motor Atık Isılarının Geri Kazanımında Termoelektrik Jeneratörlerin Kullanımı, 3(2) (2016) 192–203.

[3] The Doha Metro – Tunnelling in special Dimensions, (2012).

[4] Y. F. GORGULU, Generating Electrical Energy by Using Air Flow Occurrence in Underground Metros, Oxford Brookes University, (2015).
[5] Doha Metro. [Online]. Available: https://corp.qr.com.qa/English/Projects/Pages/DohaMetro.aspx. [Accessed: 20-Feb-2020].
[6] A. Kalmikov and K. Dykes, Wind Power Fundamentals, (2017).
[7] Sumukh Kulkarni, Abhay Badhe, Prashant Kumbhar, Prem Panaval, Rohit Jadhao, Experimental Validation of Computational Design of Wind Turbine with Wind Lens SSRG International Journal of Mechanical Engineering 6(5) (2019): 9-13.
[8] 'Aelos Wind Turbine'. [Online]. Available: https://www.windturbinestar.com/1kwv-v-aeolos-wind-turbine.html. [Accessed: 20-Feb-2020].
[9] S. Krohn, P.-E. Morthorst, and S. Awerbuch, The Economics of Wind Energy, 2009.
[10] Qatar electricity prices, June 2019 | GlobalPetrolPrices.com. [Online]. Available: https://www.globalpetrolprices.com/Qatar/electricity_prices/. [Accessed: 20-Feb-2020].
[11] Y. F. Gorgulu et al., Generating Electrical Energy by Using Air Flow Occurrence on Horizontal Wind Turbines in Underground Metros ; A Case Study in London, 1258–1266.
[12] High efficiency wind turbine based on jet engine technology, (2008). [Online]. Available: https://newatlas.com/flodesign-high-efficiency-wind-turbine-based-on-jet-engine-technology/10556/. [Accessed: 20-Feb-2020].